vacuum. A solution of an excess of CNCO-*t*-Bu (3–4 equiv) in 30 mL of CH_2Cl_2 was added at −40 °C to the (TPP)Fe^{II} complex previously prepared. After a reaction time of 10 min, complex **2** was precipitated by addition of 60 mL of deaerated CH_3OH (yield 0.098, 78%). Mass spectrum, *m/e*: 668 [(TPP)Fe], 111 (CNCO-*t*-Bu).

Complex 1 was prepared as described above. Yield: 85%. Anal. Calcd for $C_{60}H_{38}N_6O_2Fe$: C, 77.41; H, 4.09; N, 9.03. Found: C, 77.82; H, 4.35; N, 8.71.[11]

Synthesis of Complexes 3 and 4. Both complexes were prepared as described above, except only 1 equiv of the N-functionalized isocyanide was added. As shown by IR spectroscopy, products obtained in crystalline form contain the pentacoordinate species (≃90%) contaminated with the hexacoordinate species.

General Procedure for Preparation of Complexes 5–8. Addition of a base L (1 equiv in CH_2Cl_2 (5 mL) to (TPP)Fe(CNCOPh)$_2$ (0.2 g) in CH_2Cl_2 (20 mL) under argon gave rapidly (5–20 mn) the expected complexes (TPP)Fe(CNCOPh)(L), which have been crystallized by CH_3OH addition (80 mL). **5**: yield 92%. Anal. Calcd for $C_{57}H_{38}N_6OFe$: C, 77.97; H, 4.33; N, 9.57. Found: C, 77.31; H, 4.21; N, 9.10). **6**: yield 83%; mass spectrum, *m/e* 668 [(TPP)Fe], 131 (CN-COC_6H_5), 79 (py). **7**: yield 78%; mass spectrum, *m/e* 668 [(TPP)Fe], 131 ($CNCOC_6H_5$), 104 (4-CNpy). 8: yield 59%; mass spectrum, *m/e* 668 [(TPP)Fe], 131 ($CNCOC_6H_5$), 88 (THT); reaction time 4 h.

Complexes 9 and 10 were prepared as described above by using *meso*-tetratolylporphyrin instead of *meso*-tetraphenylporphyrin. **9**: yield 87%. **10**: yield 83%. Anal. Calcd for $C_{61}H_{46}N_6OFe$: C, 78.36; H, 4.96; N, 8.99. Found: C, 77.52; H, 4.93; N, 9.20.

Synthesis of Complex 11. A solution of 0.1 g of (DPDME)$Fe^{III}Cl$ in 50 mL of CH_2Cl_2/H_2O (4/1) was reduced under argon by sodium dithionite (10 min).[13] The solution was then decanted, and an excess of CNCOPh (3 equiv) in 30 mL of CH_2Cl_2 was added at 0 °C to the (DPDME)Fe^{II} prepared. After the mixture was stirred for 10 min, the solution was concentrated to 10 mL of CH_2Cl_2. Addition of 40 mL of pentane yielded crystals of the expected complex (DPDME)Fe^{II}-(CNCOPh)$_2$: yield 0.08 g; mass spectrum, *m/e* 586 [(DPDME)Fe], 131 (CNCOPh).

Complex 12 was prepared by the same procedure: yield 78% of (DPDME)Fe(CNCO-*t*-Bu)$_2$; mass spectrum, *m/e* 586 (DPDME), 111 (CNCO-*t*-Bu).

Synthesis of Complex 13. Addition of 1 equiv of pyridine (10 mg) in 10 mL of CH_2Cl_2 to (DPDME)Fe(CNCOPh)$_2$ (0.1 g) in 20 mL of CH_2Cl_2 under argon gave immediately the expected product (DPDME)Fe(CNCOPh)(py).

Acknowledgment. We thank Professor F. Varret for his contribution to the Mössbauer work.

Contribution from the Department of Chemistry, Northwestern University, Evanston, Illinois 60201, Istituto di Chimica e Tecnologia di Radioelementi, CNR, 35100 Padua, Italy, Dipartimento di Chimica, Universita di Catania, 95125 Catania, Italy, and Department of Chemistry, The Ohio State University, Columbus, Ohio 43210

Combined He I/He II Photoelectron Spectroscopic and Hartree–Fock–Slater Investigation of Electronic Structure and Bonding in Uranium Hexamethoxide

B. E. Bursten,*[1a,b] M. Casarin,*[1c] D. E. Ellis,*[1d] I. Fragalà,*[1e] and T. J. Marks*[1d]

Received October 7, 1985

The electronic structure of the uranium(VI) alkoxide $U(OCH_3)_6$ has been investigated by using a combination of He I/He II photoelectron spectroscopy and discrete variational (DV) Xα molecular orbital calculations. Good agreement is obtained between the experimental and calculated ionization energies. It is found that the low ionization energy features of the photoelectron spectra are due to varying degrees of donation of the oxygen lone pairs to the empty orbitals on the uranium atom and to the reduction of the molecular symmetry to C_i via bending of the U–O–C linkages. The methyl groups act as both σ and π donors to the oxygen 2p orbitals, increasing the overall donor strength of the alkoxide ligands.

Introduction

The bonding characteristics of actinide alkoxides[2] are of current interest for a number of reasons. First, M–OR functionalities are frequently endproducts in a variety of reactions involving organoactinide alkyls and hydrides,[3] and the driving force to produce such products is frequently unclear. Second, and closely connected with the first reason, molecular structural studies[3,4] have

(1) (a) The Ohio State University. (b) Camille and Henry Dreyfus Teacher-Scholar (1984–1989) and Fellow of the Alfred P. Sloan Foundation (1985–1987). (c) Istituto di Chimica e Tecnologia di Radioelementi. (d) Northwestern University. (e) Universita di Catania.

(2) For recent reviews of actinide alkoxide compounds, see: (a) "Gmelins Handbook of Inorganic Chemistry", 8th ed.; Springer Verlag: West Berlin, 1983; Vol. C13, Supplement, Uranium, pp 50–96. (b) Bradley, D. C.; Mehrotra, R. C.; Gaur, D. P. "Metal Alkoxides"; Academic Press: New York, 1978; pp 116–134. (c) Bradley, D. C. *Adv. Inorg. Chem. Radiochem.* **1972**, *15*, 259–322. (d) Bradley, D. C.; Fisher, K. J. *MTP Int. Rev. Sci.: Inorg. Chem., Ser. One* **1972**, *5*, 65–78.

(3) (a) Duttera, M. R.; Day, V. W.; Marks, T. J. *J. Am. Chem. Soc.* **1984**, *106*, 2907–2912. (b) Duttera, M. R.; Marks, T. J., manuscript in preparation. (c) Moloy, K. G.; Marks, T. J. *J. Am. Chem. Soc.* **1984**, *106*, 7051–7064 and references therein. (d) Sonnenberger, D. C.; Mintz, E. A.; Marks, T. J. *J. Am. Chem. Soc.* **1984**, *106*, 3484–3491. (e) Marks, T. J.; Ernst, R. D. In "Comprehensive Organometallic Chemistry"; Wilkinson, G. W.; Stone, F. G. A., Abel, E. W., Eds.; Pergamon Press: Oxford, 1982; Chapter 21. (f) Marks, T. J. *Science* (Washington, D.C.) **1982**, *217*, 989–997. (g) Marks, T. J., Day, V. W. In "Fundamental and Technological Aspects of Organo-f-Element Chemistry"; Marks, T. J., Fragalà, I. L., Eds.; D. Reidel: Dordrecht, The Netherlands, 1985; pp 115–157.

Table I. Photoelectron Spectroscopic Data, Band Assignments, and Calculated Transition-State Ionization Energies of $U(OCH_3)_6$

band label	exptl IE,[a] eV	rel intens[b] He I	rel intens[b] He II	assignt	calcd IE, eV
a	8.80	1.00	1.00	$22a_g$	7.64
				$24a_u$	(7.69)[c]
				$21a_g$	(7.80)
a′	9.30	1.05	0.95	$23a_u$	(8.20)
				$20a_g$	(8.37)
b	9.95	1.10	1.75	$19a_g$	(8.77)
				$22a_u$	8.77
				$21a_u$	(9.22)
				$20a_u$	(9.33)
c	10.74	0.75	0.70	$18a_g$	9.70
				$17a_g$	(9.32)
d	12.79	0.50	0.45	$19a_u$	10.52
e	14.83	3.10	2.80	U–O and C–H σ bonds	

[a] Peak energies refer to centroids of Gaussian components. [b] Arbitrary units corrected for the analyzer transmission function. [c] Values in parentheses are estimated from ground-state values by using the energy shift of similar orbitals.

0020-1669/86/1325-1257$01.50/0

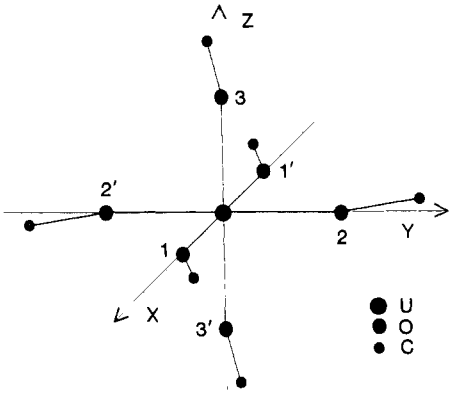

Figure 1. Molecular structure of $V(OCH_3)_6$ and coordinate system and numbering scheme used for $U(OCH_3)_6$.

revealed distinctive metrical parameters (i.e., large M–O–R angles and short M–O distances) that suggest unusual metal–ligand bonding modes. Third, volatile uranium alkoxide complexes such as $U(OCH_3)_6$ represent successful prototypes for the 10.6-μm infrared laser-induced multiphoton separation of isotopes ^{235}U and ^{238}U.[5,6] Electronic structural information is essential to an in-depth understanding of $U(OCH_3)_6$ photophysical processes. Last, a description of the bonding in actinide alkoxide molecules represents a further step in quantum chemical complexity beyond simple actinide carbides, halides, and oxides and as such will provide valuable insight with regard to the reliability of approximate and ab initio methodology applied to such systems.

In this contribution, we focus upon the uranium hexamethoxide molecule, $U(OCH_3)_6$, in a combined experimental and theoretical study using both gas phase He I/He II photoelectron spectroscopy (PES) and Xα molecular orbital calculations in the discrete variational (DV) formalism. The $U(OCH_3)_6$ molecule has already been characterized by a variety of physical techniques, including X-ray diffraction.[5,6] This contribution represents the first combined PES/DV-Xα study of any actinide complex and the first experimental/theoretical electronic structural study of an actinide alkoxide. It will be seen that excellent agreement is obtained between experiment and theory and that significant new information is obtained about the metal–ligand bonding.

Experimental and Computational Section

Experimental Methods. $U(OCH_3)_6$ was prepared according to the literature procedure.[6a] It was purified by multiple sublimation under high vacuum and gave satisfactory ^1H NMR and mass spectrometric analyses. It was handled at all times under inert atmosphere by standard techniques. The photoelectron spectra were recorded on a Perkin-Elmer PS 18 spectrometer modified by the inclusion of a hollow-cathode discharge source giving high output of He II photons (Helectros Development Corp.). The spectra were accumulated in the "multiple scan mode" with the aid of a MOSTEK computer directly interfaced to the spectrometer. The energy scale of consecutive scans was locked to the reference values of the Ar $^2P_{3/2}$ ionization and the He $(1s)^{-1}$ self-ionization.

Deconvolution of the spectra was carried out by fitting the experimental profiles with a series of asymmetric Gaussian functions after subtraction of background. The areas of bands thus evaluated are estimated to be accurate to better than 5%. The relevant PES data and proposed assignments are given in Table I.

Computational Methods. Electronic structure calculations were of the discrete variational (DV) Xα type.[7] The molecular electron density was approximated with an s-wave expansion (overlapping spherical functions on every center) in calculating the potential, and the SCF equations were converged by a self-consistent charge (SCC) procedure,[7] which has already been found to give a fairly good description of the molecular potential in actinide carbides, halides, and oxides.[8] Atomic coordinates for $U(OCH_3)_6$ were taken directly from the solid-state structure of the molecule as determined by X-ray diffraction.[6b] The UO_6 framework of $U(OCH_3)_6$ is of essentially octahedral symmetry (Figure 1) with mean values for the U–O and O–C bond lengths of 2.10 and 1.35 Å, respectively. The mean U–O–C angle is 153.7°. The molecular symmetry in the crystalline state belongs to the C_i point group.

The variational basis for the uranium atom consisted of nonrelativistic numerical atomic orbitals (AO) of the doubly charged ion corresponding to an electronic configuration of $(Rn)5f^36s^26p^66d^17s^07p^0$. A potential well with internal and external radii equal to 4.0 and 6.0 a. u., respectively, and with a depth of 2.0 Ry was added to the atomic potential for further localization of the diffuse valence states.[7a] Several numerical experiments were first performed on the simpler model compound $U(OH)_6$ in an effort to identify the best basis set for the oxygen atoms. The molecular energy levels obtained from an SCC calculation using an extended basis set for neutral oxygen atoms (including 3s and 3p AOs) gave an overall shift toward higher binding energy of ca. 3 eV with respect to the minimal basis set. The critical factor in this rather large change was seen to be the increased overlap between the uranium-centered AOs and oxygen AOs. To allow the use of a minimal basis set in the full-scale calculations, we introduced some negative charge on the oxygen atoms. Thus, the initial oxygen electronic population was increased to allow greater spatial extension of the 2p AOs, resulting in an improved overlap with the uranium AOs. The starting ionicity that best reproduced the extended basis set results was −0.7. A total of 7532 integration points were used to determine the Hamiltonian and overlap matrix elements in the self-consistent calculations on $U(OCH_3)_6$. The numerical precision of the Hamiltonian matrix elements is estimated to be better than 0.1 eV. The exchange scaling parameter α was set equal to $^2/_3$ throughout the calculations. To evaluate the magnitude of electronic relaxation associated with the removal of one electron from the various ground state MOs, ionization energy calculations were carried out by using Slater's transition-state formalism.[9]

The calculated ionization energy values are compared to the experimental data in Table I. It is found that, despite great differences in the ground-state atomic composition of the high-lying MOs, the relaxation effects are similar for all of them, ranging from 1.5 to 2.0 eV. The theoretical ionization energies are underestimated by 1.2–2.3 eV, the discrepancy increasing with the binding energy. This shift and compression of the computed valence PES features is at least partially due to the neglect of relativistic effects (spin–orbit splitting and indirect shielding effects on the U 5f component) and the omission of anisotropic potential terms in the SCC procedure.

Discussion

As was the case for other octahedral U(VI) complexes, e.g. UF_6[10] and UCl_6,[11] we expect the highest lying orbitals of $U(OCH_3)_6$ to consist primarily of lone-pair orbitals on the ligands. These will be split through interactions with the various available empty orbitals on the U atom and by ligand–ligand repulsions. We shall direct our discussion first toward understanding the

(4) (a) Cotton, F. A.; Marler, D. O.; Schwotzer, W. *Inorg. Chim. Acta* **1984**, *95*, 207–209. (b) Cotton, F. A.; Marler, D. O.; Schwotzer, W. *Inorg. Chim. Acta* **1984**, *85*, L31–32. (c) Miller, S. S. Ph.D. Thesis, Northwestern University, 1980, Molecular structure of $\{U[OC(CH_3)_3]_5\}_2$. (d) Marks, T. J.; Manriquez, J. M.; Fagan, P. J.; Day, V. W.; Day, C. S.; Vollmer, S. H. *ACS Symp. Ser.* **1980**, *No. 131*, 1–29.

(5) (a) Cuellar, E. A.; Miller, S. S.; Marks, T. J.; Weitz, E. *J. Am. Chem. Soc.* **1983**, *105*, 4580–4589. (b) Cuellar, E. A.; Miller, S. C.; Teitelbaum, R. C.; Marks, T. J.; Weitz, E. In "Progress in Rare Earth Science and Technology. III;" Silber, H. S.; Rhyne, J. J., Eds.; Plenum Press: New York, 1982; pp. 71–76. (c) Miller, S. S.; DeFord, D. D.; Marks, T. J.; Weitz, E. *J. Am. Chem. Soc.* **1979**, *101*, 1036. (d) Coleman, J. H.; Marks, T. J. U.S. Patent 4,097,384, 1978. (e) Cuellar, E. A.; Marks, T. J.; Miller, S. S.; Weitz, S. U.S. Patent 4,364,870, 1982.

(6) (a) Cuellar, E. A.; Marks, T. J. *Inorg. Chem.* **1981**, *20*, 2129–2137. (b) Miller, S. S.; Day, V. W.; Marks, T. J., manuscript in preparation.

(7) (a) Averill, F. W.; Ellis, D. E. *J. Chem. Phys.* **1973**, *59*, 6411–6418. (b) Rosen, A.; Ellis, D. E.; Adachi, H.; Averill, F. W. *J. Chem. Phys.* **1976**, *65*, 3629–3634 and references therein. (c) Trogler, W. C.; Ellis, D. E.; Berkowitz, J. *J. Am. Chem. Soc.* **1979**, *101*, 5896–5901.

(8) (a) Ellis, D. E. In "Actinides in Perspective"; Edelstein, N. H., Ed.; Pergamon Press: Oxford, 1982, pp 123–141 and references therein. (b) Ellis, D. E.; Rosen, A.; Gubanov, V. A. *J. Chem. Phys.* **1982**, *77*, 4051–4060 and references therein.

(9) Slater, J. C. "Quantum Theory of Molecules and Solids. The Self-Consistent Field for Molecules and Solids"; McGraw-Hill: New York, 1974; Vol. 4.

(10) (a) Koelling, D. D.; Ellis, D. E.; Bartlett, R. J. *J. Chem. Phys.* **1976**, *65*, 3331–3340. (b) Boring, M.; Moskowitz, J. W. *Chem. Phys. Lett.* **1976**, *38*, 185–187 and references therein. (c) Martensson, N.; Malmquist, P. A.; Svensson, S. *Chem. Phys. Lett.* **1983**, *100*, 375–377. (d) Martensson, N.; Malmquist, P. A.; Svensson, S.; Johansson, B. *J. Chem. Phys.* **1984**, *80*, 5458–5464. (e) Larsson, S.; Tse, J. S.; Esquivel, J. L.; Tang Kai, A. *Chem. Phys. Lett.* **1984**, *109*, 43–47.

(11) Thornton, G.; Edelstein, N.; Rösch, N.; Egdell, R. G.; Woodwark, D. R. *J. Chem. Phys.* **1979**, *70*, 5218–5221.

Table II. Unnormalized Symmetry-Adapted Linear Combinations of the Oxygen π Orbitals of $U(OCH_3)_6$ under Octahedral Symmetry and the Character of Each after Symmetry Reduction

representation under O_h	unnormalized SALCs	character after reduction to C_i
t_{1g}	$y_1 - y_{1'} - x_2 + x_{2'}$	σ
	$z_1 - z_{1'} - x_3 + x_{3'}$	$\sigma + \pi$
	$z_2 - z_{2'} - y_3 + y_{3'}$	π
t_{1u}	$x_2 + x_{2'} + x_3 + x_{3'}$	σ
	$y_1 + y_{1'} + y_3 + y_{3'}$	$\sigma + \pi$
	$z_1 + z_{1'} + z_2 + z_{2'}$	π
t_{2g}	$y_1 - y_{1'} + x_2 - x_{2'}$	σ
	$z_1 - z_{1'} + x_3 - x_{3'}$	$\sigma + \pi$
	$z_2 - z_{2'} + y_3 - y_{3'}$	π
t_{2u}	$x_2 + x_{2'} - x_3 - x_{3'}$	σ
	$y_1 + y_{1'} - y_3 - y_{3'}$	$\sigma + \pi$
	$z_1 + z_{1'} - z_2 - z_{2'}$	π

effects of reducing the symmetry from O_h to C_i.

Each OCH_3^- ligand can be qualitatively considered as containing three lone-pair orbitals, one collinear with the O–C axis of a_1 symmetry, and a doubly degenerate pair of e symmetry under C_{3v}. Were all of the U–O–C linkages perfectly linear, these lone-pairs would, of course, divide into a set of six σ lone pairs ($a_{1g} + e_g + t_{1u}$ under O_h symmetry) and a set of 12 π lone pairs ($t_{1g} + t_{2g} + t_{1u} + t_{2u}$ under O_h symmetry). It is expected that the σ set will interact most strongly with the U atom, resulting in MOs of a_{1g}, e_g, and t_{1u} symmetry, which will be relatively lower lying than the set of π orbitals. We shall, therefore, concentrate on the π orbitals for now, assuming first that the U–O–C linkages are linear and then seeing the effects of allowing these to bend.

Of the four triply degenerate sets of π orbitals, the t_{2g} is of appropriate symmetry to interact with the empty 6d orbitals of the U atom, the t_{2u} can interact with the 5f orbitals, and the t_{1g} cannot interact with any of the low-lying U orbitals. The t_{1u} can interact with the 5f and 7p orbitals of the U atom, but it will also interact and compete with the t_{1u} set of σ orbitals when allowed to do so by the presence of the U atom. Qualitatively, therefore, the t_{2u} and t_{2g} orbitals should be most stabilized by donation to the metal, the t_{1g} will be entirely nonbonding, and the t_{1u} will be stabilized by donation but destabilized by interactions with the σ set. As will be seen, this qualitative ordering is indeed followed, although the picture is complicated by the reduction of symmetry.

With reference to the coordinate system and numbering scheme shown in Figure 1, Table II lists the unnormalized symmetry-adapted linear combinations (SALCs) of the π orbitals of the six O atoms that comprise the four triply degenerate representations. The distortions from octahedral symmetry can be thought of as moving C1 and C1′ in the xy plane, C2 and C2′ in the xy plane, and C3 and C3′ in the xz plane. Thus, the p_z orbitals on O1, O1′, O2, and O2′ and the p_y orbitals on O3 and O3′ remain purely π in character since they are perpendicular to the planes defined by the U–O–C linkages. The remaining orbitals (p_y on O1 and O1′, p_x on O2, O2′, O3, and O3′) are, in a sense, rehybridized by mixing with the set of σ lone pairs and with the O–C σ bonds. They will be directed away from the U atom and hence will overlap less effectively with it than will the pure π lone pairs. They will also be destabilized relative to the pure π orbitals since they are the antibonding combination resulting from the interaction of the σ and π orbitals. This set of rehybridized lone pairs, which we will refer to as "σ-oids", can be thought of as arising from a rehybridization of the O atoms from sp, as would be the case for linear U–O–C bonds, to a limiting hybridization of sp^2, which would be expected if the U–O–C bond angles were 120°.

As shown in Table II, each of the set of triply degenerate π orbitals will partition itself upon bending of the U–O–C linkage. One of the combinations consists entirely of pure π oribtals, one consists entirely of σ-oids, and one has equal contributions from each and is hence labeled $\sigma + \pi$. Since the π orbitals are spatially better able to interact with the uranium atom than are the σ-oids, we expect the extent of interaction in each set to follow the order $\pi > \sigma + \pi > \sigma$. The stabilization of each lone-pair orbital should also follow this order, and thus, for each set of three SALCs, we would expect the π to be lowest in energy, the σ highest, and the $\sigma + \pi$ intermediate.

Table III. Calculated Ground-State Orbital Energies (eV) and Population Analyses (%) for the 12 Highest Occupied Molecular Orbitals of $U(OCH_3)_6$

MO sym							O		
C_i	O_h	$-E$	U(5f)	U(6d)	U(p)	U(s)	π	σ	(CH_3)
$22a_g$	t_{1g}	5.96	0	0	0	0	1	68	31
$24a_u$	t_{1u}	6.01	16	0	5	0	10	44	25
$21a_g$	t_{1g}	6.09	0	2	0	0	14	57	27
$23a_u$	t_{1u}	6.41	15	0	5	0	19	39	22
$20a_g$	t_{1g}	6.54	0	0	0	0	78	0	22
$19a_g$	t_{2g}	6.85	0	11	0	0	0	48	41
$22a_u$	t_{2u}	6.93	36	0	0	0	4	28	32
$21a_u$	t_{2u}	7.29	26	0	1	0	43	9	21
$20a_u$	t_{2u}	7.42	17	0	3	0	54	6	20
$18a_g$	t_{2g}	7.67	0	9	0	0	61	5	26
$17a_g$	t_{2g}	7.84	0	10	0	0	56	0	34
$19a_u$	t_{1u}	8.98	6	0	5	0	31	14	44

Table III lists the DV-Xα derived orbital energies and population analyses of the highest occupied molecular orbitals of $U(OCH_3)_6$. Also given is the approximate O_h "parentage" of each of the orbitals. It is seen that the $20a_g$, $21a_g$, and $22a_g$ orbitals, which we correlate with the nonbonding t_{1g} set, show a negligible interaction with the metal. The three orbitals are split by ca. 0.6 eV, a consequence of the relatively higher energy of the σ-oids vis-ã-vis the π orbitals. The $20a_u$, $21a_u$, and $22a_u$ orbitals, which are derived from the t_{2u} set under O_h symmetry, strongly donate to the U 5f orbitals, as expected, and exhibit a splitting comparable to that of the t_{1g}. The $17a_g$, $18a_g$, and $19a_g$ orbitals, all derived from the t_{2g} set, show similar behavior although the splitting of about 1.0 eV is greater than that of the preceding two. The $19a_u$, $23a_u$, and $24a_u$ show appreciable interaction with both of the U 5f and 6p atomic orbitals, indicative that these three orbitals have their origin in the t_{1u} set of lone pairs. In contrast to the t_{1g}, t_{2g}, and t_{2u} orbitals, the t_{1u} set shows a very large splitting of ca. 3.0 eV. This is due to extensive mixing of these orbitals with the t_{1u} orbitals of σ symmetry. It is clear, though, that, with the exception of the t_{1u} set, the ordering of the orbitals and the magnitude of the splitting is in accord with our qualitative notions.

When the symmetry is reduced from O_h to C_i, it is no longer necessary that the symmetries of the oxygen π orbitals adapt themselves as given in Table II. Table IV gives the composition of each of the lone-pair orbitals in $U(OCH_3)_6$ in terms of the oxygen 2p orbitals (referenced to the master coordinate system). It can be seen that extensive rearrangement of the 2p contributions does occur. In particular, the four $\sigma + \pi$ orbitals mix among themselves to produce two orbitals ($21a_g$ and $23a_u$) that are predominantly σ-oid in character and two orbitals ($18a_g$ and $21a_u$) that are predominantly π.

The higher energy of the σ-oid orbitals relative to the pure π orbitals is also consistent with a significant interaction of the O–C σ bonds with the O π orbitals in the U–O–C planes upon reducing the symmetry to C_i; since the O–C σ bonds are lower in energy than the O 2p orbitals, such an interaction will have the effect of destabilizing the σ-oids relative to the pure π orbitals, which are perpendicular to the U–O–C planes. Table III indicates that all of the "O lone-pair" orbitals contain a 20–44% contribution from the methyl groups. Furthermore, it is interesting to note that the interaction between the σ-oid MOs and the filled π combination of the C–H bonds[12] has the secondary effect of enhancing the ability of the oxygen atoms to act as π donors[13] to the uranium atom. That CH_3 is acting as a significant π donor to the oxygen atoms is also evident in Table III, wherein it can be seen that even the pure π orbitals (e.g., the $20a_g$ orbital) contain

(12) Hoffmann, R.; Radom, L.; Pople, J. A.; Schleyer, P. v. R.; Hehre, W. J.; Salem, L. *J. Am. Chem. Soc.* **1972**, *94*, 6221–6223 and references therein.

(13) DeFrees, D. J.; Bartmess, J. E.; Jhong, K. K.; McIver, R. T., Jr.; Hehre, W. J. *J. Am. Chem. Soc.* **1977**, *99*, 6451–6452.

Table IV. Oxygen 2p Atomic Orbital Contributions (%) to the Pseudo-Lone-Pair Molecular Orbitals of $U(OCH_3)_6$[a]

sym		O1, O1′			O2, O2′			O3, O3′			
C_i	O_h	p_x	p_y	p_z	p_x	p_y	p_z	p_x	p_y	p_z	nature
$22a_g$		2	27	1	33	2	0	3	0	1	σ
$21a_g$	t_{1g}	0	1	14	2	0	0	52	0	2	σ
$20a_g$		0	0	0	0	0	37	0	41	0	π
$24a_u$		3	0	5	17	0	5	22	0	2	σ
$23a_u$	t_{1u}	1	34	1	0	4	4	0	14	0	σ
$19a_u$		2	0	3	3	0	28	0	0	9	π
$19a_g$		1	33	0	14	0	0	0	0	0	σ
$18a_g$	t_{2g}	0	0	61	0	0	0	5	0	0	π
$17a_g$		0	0	0	0	0	26	0	30	0	π
$22a_u$		0	2	0	13	0	4	13	0	0	σ
$21a_u$	t_{2u}	0	7	0	1	1	0	0	43	0	π
$20a_u$		0	0	55	0	0	0	3	0	2	π

[a] Each symmetry set is given in order of decreasing energy.

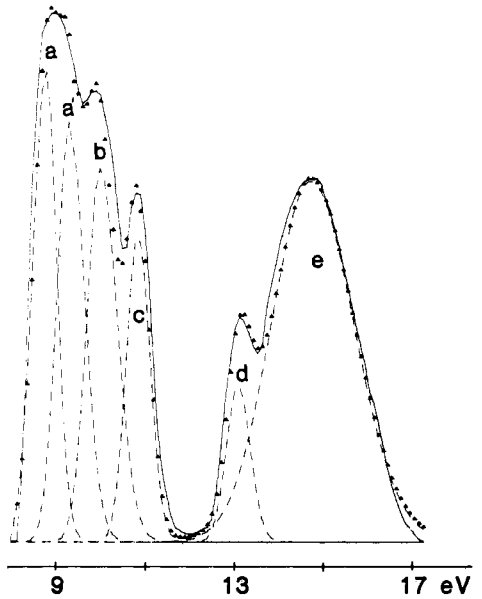

Figure 2. 8–18 eV ionization energy region of the He I photoelectron spectrum of $U(OCH_3)_6$.

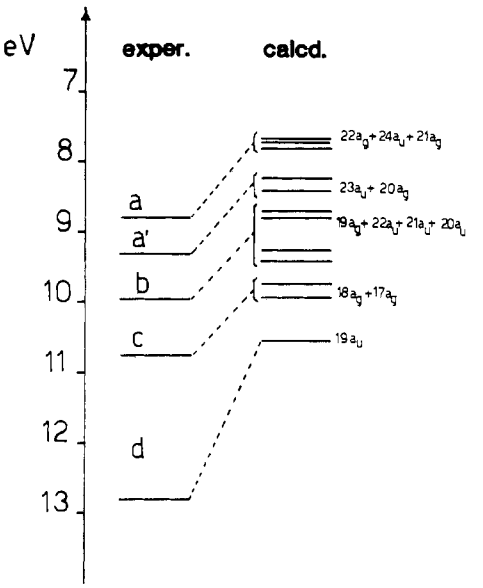

Figure 3. Comparison between the experimental and the computed transition-state ionization energies of $U(OCH_3)_6$.

significant contributions from the methyl groups. It is important to point out that the aforementioned π-donor interaction provides a convincing explanation for the unusually large M–O–C angles found in many metal alkoxides,[2-4] including the present one[6]; as the strength of the proposed π interaction increases, so will the tendency toward a linear M–O–C linkage increase. Thus, we see that the methyl groups of the methoxide ligands are acting as both σ- and π-electron donors.

The He I PE spectrum of $U(OCH_3)_6$ is shown in Figure 2. It consists of five well-resolved bands (labeled a, b, c, d, and e) in the 8–18 eV ionization region. Deconvolution of the experimental PES profiles was performed for bands up to 18 eV, and the relative band areas were corrected for the analyzer transmission function. The best fit is obtained by using six asymmetric Gaussian components (a, a′, b, c, d, and e) having the relative intensity ratios compiled in Table I. These general features correlate quite well with the Xα molecular orbital energies (Table III), although the eigenvalues are uniformly too high by ca. 3 eV, as is frequently found for ground-state Xα calculations.[8b,14] As might be expected, a better absolute agreement is found between the calculated transition state IPs, given in Table I, and the experimental IPs.

Figure 3 illustrates our proposed assignment of the orbital ionizations accounting for each band of the experimental spectrum. On the basis of both the relative intensities and the foregoing theoretical results, the components a and a′ must be assigned to

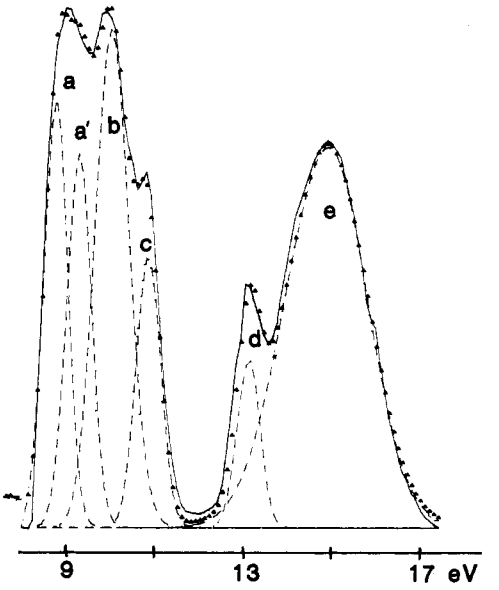

Figure 4. 8–18 eV ionization energy region of the He II photoelectron spectrum of $U(OCH_3)_6$.

ionization of the $22a_g + 24a_u + 21a_g$ and the $23a_u + 20a_g$ MOs, respectively. The bands b and c are ascribable to ionizations of the $19a_g + 22a_u + 21a_u + 20a_u$ and the $18a_g + 17a_g$ MOs, respectively. Band d is assigned to ionization of the $19a_u$ MO solely.

(14) Bursten, B. E.; Casarin, M.; DiBella, S.; Fang, A.; Fragalà, I. *Inorg. Chem.* **1985**, *24*, 2169–2173.

The intense and broad band e cannot be assigned in great detail. It certainly contains ionizations from the U–O σ bonds and probably overlaps the O–C σ ionizations as well.

The change from He I to He II radiation produces notable changes in relative PES band intensities, as shown in Figure 4. The most striking effect is the remarkable increase in intensity of band b. This intensity increase is in accord with the calculations since the MOs that contribute to band b have the largest metal 5f contributions (Table III). Hence, if the Gelius model for PE cross sections is adopted,[15] the observed intensity change reproduces the well-known increases of the U 5f and 6d cross sections relative to those of O and C under He II excitation.[11,16] Interestingly, the relative intensities of the remaining bands of the He II spectrum are in better agreement than the He I spectrum with the statistical values based on proposed occupancies. This effect is frequently observed on passing from He I to He II spectra and could be due to a less pronounced effect of the second-order terms in the plane wave approximation for molecular photoelectron cross sections under the more energetic He II radiation.[17] It is also of interest to note that the He II intensities suggest that the increase in the U 5f cross section is slightly greater than that of the U 6d. In our previous study of Cp_4U,[14] it appeared that this order was reversed, i.e. U 6d > U 5f. We suggest that this underscores the need for additional experimental and theoretical studies of heavy-element cross sections.

(15) Gelius, V. In "Electron Spectroscopy"; Shirley, D. A.; Ed.; North-Holland Publishing Co.: Amsterdam, 1972; p 311.
(16) (a) Ciliberto, E.; Condorelli, G.; Fagan, P. J.; Manriquez, J. M.; Fragalà, I.; Marks, T. J. *J. Am. Chem. Soc.* **1981**, *103*, 4755–4759. (b) Fragalà, I. L.; Goffart, J.; Granozzi, G.; Ciliberto, E. *Inorg. Chem.* **1983**, *22*, 216–220. (c) Casarin, M.; Ciliberto, E.; Fragalà, I. L.; Granozzi, G. *Inorg. Chim. Acta* **1982**, *64*, L247–L249. (d) Down, A. J.; Egdell, R. G.; Orchard, A. F.; Thomas, P. D. P. *J. Chem. Soc., Faraday Trans. 2*, **1978**, 1755–1761. (e) Clark, J. P.; Green, J. C. *J. Chem. Soc., Dalton Trans.* **1977**, 505–508. (f) Fragalà, I. L.; Gulino, A. In "Fundamental and Technological Aspects of Organo-f-Element Chemistry"; Marks, T. J., Fragalà, I. L., Eds.; D. Reidel: Dordrecht, The Netherlands, 1985; pp 327–360.
(17) Rabalais, J. W. "Principles of Ultraviolet Photoelectron Spectroscopy"; Wiley: New York, 1977.

Conclusions

We believe that the study of the electronic structure of $U(OCH_3)_6$ presented here is significant for several reasons. It demonstrates the utility of the DV-Xα molecular orbital method for describing the bonding energetics of metal–organic actinide molecules. It also underscores our previous claim that the correct assignment of PE spectra for f-element complexes almost by necessity requires a suitable calculational description of the bonding in them.[14]

The electronic structure of $U(OCH_3)_6$ is, not surprisingly, more complex than that of truly octahedral molecules such as UX_6 (X = F, Cl). It is surprising, however, that the U(VI) center is capable of producing such a large (ca. 3–4 eV) splitting in the oxygen π orbitals. It is precisely these largely unexpected metal–ligand interactions in such systems that encourages us that the electronic structure of f-element complexes will continue to show significant variances from those of transition-metal analogues and that investigations such as the present one are essential if these variances are to be completely understood.

Acknowledgment. This research was supported by the NSF (Grants CHE8306255 to T.J.M. and DMR8214966 to D.E.E.) and by the NATO research grants program (Grant 068/84 to I.F. and T.J.M.). B.E.B. gratefully acknowledges the donors of the Petroleum Research Fund, administered by the American Chemical Society, for partial support.

Registry No. $U(OCH_3)_6$, 69644-82-2.

Contribution from the Department of Chemistry, Amherst College, Amherst, Massachusetts 01002

Thermodynamics of Azide and Thiocyanate Binding to Bovine Copper–Zinc Superoxide Dismutase

David M. Dooley* and Michele A. McGuirl

Received October 21, 1985

Thermodynamic parameters (K, $\Delta H°$, $\Delta S°$) have been measured for N_3^- and SCN^- binding to bovine copper–zinc superoxide dismutase. Comparative data have also been obtained for the anation reactions of Cu(II)–diethylenetriamine (dien). The thermodynamics of N_3^- and SCN^- binding to superoxide dismutase are very different. Moreover, the enzyme + SCN^- reaction cannot be described by a single equilibrium constant and is ionic strength dependent. However, it is clear that $\Delta S°$ is far more important in the enzyme–anion reactions as compared to $Cu(dien)^{2+}$ ligand substitution, which is dominated by $\Delta H°$.

Anion binding to bovine copper–zinc superoxide dismutase (Cu,Zn-SOD) has been extensively investigated, in part because the coordination of small anions (e.g. N_3^-, CN^-, SCN^-) may model the interaction between the enzyme and superoxide.[1] Azide and cyanide are potent inhibitors of Cu,Zn-SOD and are known to coordinate to Cu(II). Conflicting results have been reported with regard to thiocyanate binding;[2,3] Bertini and co-workers have presented evidence for imidazole (from a nonbridging histidine) displacement by anions, including SCN^-,[2] but this has been disputed.[3] In contrast to N_3^- and CN^-, SCN^- binding does not perturb the solvent water ^1H NMR T_1.[2] SCN^- has been shown to displace the bridging imidazolate in the 4-Cu derivative of Cu,Zn-SOD.[4] Thus, it seems likely that SCN^- binds differently than N_3^- and CN^-. In addition, the fact that phosphate has recently been shown to inhibit Cu,Zn-SOD and to influence its reactivity toward potential Cu(II) ligands[5] complicates the interpretation of previous work carried out in phosphate buffers. Although some equilibrium constants for anion binding to bovine Cu,Zn-SOD have been reported[1-6], $\Delta H°$ and $\Delta S°$ have not been determined. Such thermodynamic data are essential to under-

(1) (a) Valentine, J. S.; Pantoliano, M. W. In *Copper Proteins*; Spiro, T. G., Ed.; Wiley: New York, 1980; pp 291–358. (b) Fielden, E. M.; Rotilio, G. In *Copper Proteins and Copper Enzymes*; Lontie, R., Ed.; CRC: Boca Raton, FL, 1984; Vol. II, pp 27–61.
(2) (a) Bertini, I.; Luchinat, C.; Scozzafava, A. In *The Coordination Chemistry of Metalloenzymes*; Bertini, I., Drago, R. S., Luchinat, C., Eds.; D. Reidel: Boston, 1983; pp 155–158. (b) Bertini, I.; Luchinat, C.; Scozzafava, A. *J. Am. Chem. Soc.* **1980**, *102*, 7349–7353. (c) Bertini, I.; Lanini, G.; Luchinat, C.; Messori, L.; Monnanni, R.; Scozzafava, A. *J. Am. Chem. Soc.* **1985**, *107*, 4391–4396.
(3) (a) Calabrese, L.; Cocco, D.; Rotilio, G. In *Oxy Radicals and Their Scavenger Systems*; Vol. I, Cohen, G., Greenwald, R. A., Eds.; Elsevier: New York, 1983; Vol. I, pp 179–186. (b) Rotilio, G. In *The Coordination Chemistry of Metalloenzymes*; Bertini, I.; Drago, R. S.; Luchinat, C., Eds.; D. Reidel: Boston, 1983; pp 147–154.
(4) Strothkamp, K. G.; Lippard, S. J. *Biochemistry* **1981**, *20*, 7488–7493.
(5) Mota de Freitas, D.; Valentine, J. S. *Biochemistry* **1984**, *23*, 2079–2082.
(6) (a) Bermingham-McDonogh, O.; Mota de Freitas, D.; Kumamoto, A.; Saunders, J. E.; Blech, D. M.; Borders, C. L., Jr.; Valentine, J. S. *Biochem. Biophys. Res. Commun.* **1982**, *108*, 1376–1382. (b) Cocco, D.; Manelli, I.; Rossi, L.; Rotilio, G. *Biochem. Biophys. Res. Commun.* **1983**, *111*, 860–864.

0020-1669/86/1325-1261$01.50/0